



Invited lecture/Scientific

Reconfiguration of Nematic Dislocations

Harkai Saša¹, Kralj Mitja², Kralj Samo^{3,4,*}

1. Faculty of Mathematics and Physics, University of Ljubljana, Ljubljana, Slovenia
2. ŠKUC, Ljubljana, Slovenia
3. Faculty of Natural Sciences and Mathematics, University of Maribor, Maribor, Slovenia
4. Solid State Department, Jožef Stefan Institute, Ljubljana, Slovenia
- * Correspondence: Samo Kralj; samo.kralj@um.si

Abstract:

Basic natural entities seem to be physical fields. From this perspective elementary particles should correspond to robust localized field configurations. Most probable candidates for such configurations are topological defects. They are topologically protected and they exhibit robust body-like features. Particularly adequate structures are line defects which could display also linked or knotted configurations. Such structures could be relatively easily created, manipulated and observed in nematic liquid crystals. In this contribution we focus on nematic elementary line defects characterised by winding number $|m|=1/2$. We illustrate that they behave as line-like robust elastic objects. However, they could be reconfigured into qualitatively different conformations where topological conservation rules are obeyed.

Citation: Harkai S, Kralj M, Kralj S. Fields, Reconfiguration of nematic dislocations. Proceedings of Socratic Lectures. 2023, 8; 132-139.
<https://doi.org/10.55295/PSL.2023.I19>

Publisher's Note: UL ZF stays neutral with regard to jurisdictional claims in published maps and institutional affiliations.

Keywords: Fields; Topological defects; Topological charge; Disclinations; Liquid crystals



Copyright: © 2023 by the authors. Submitted for possible open access publication under the terms and conditions of the Creative Commons Attribution (CC BY) license (<https://creativecommons.org/licenses/by/4.0/>).



1. Introduction

Recent decades evidences that topology dominates natural behavior. It seems that key ideas introduced by Greeks and in particular by Einstein are correct: all fundamental laws of physics could be interpreted in terms of geometry. It might well be that all integers present in nature have a topological origin, i.e., they embody a topological invariant.

Topology (Kamien, 2022) deals with systems' properties which remain conserved in continuous geometrical or physical field transformations. These properties are reflected in topological invariants which are countable, discrete and conserved entities. Note that conserved quantities form the foundation of our physical understanding of the world. Topological properties reflect a global system's property, which is consequently robust and in general insensitive to local system's configurational changes. For example, a topological equivalence relates a coffee cup (Fig. 1a) and a doughnut, i.e. torus (Fig. 1b): both have in common one hole. The latter represent the topological invariant g (the so called *genus*) where $g=1$ fingerprints the toroidal topology.

Topological phenomena are relatively well understood in effectively two-dimensional (2D) manifolds (Singer, 1982) where mathematical treatment is relatively simple. Here manifold refers to a topological space, that is in general curved, that resembles Euclidian space near each point. Hence, n -dimensional curved manifold has a neighborhood that could be continuously morphed to the n -dimensional Euclidian space. For example, Gauss-Bonnet and Poincare-Hopf theorems (Kamien, 2022) relate the integrated Gaussian curvature of a closed 2D surface within a 3D system with the surface's Euler characteristics $\chi = 2(1 - g)$ and the total winding number m of the ordering field within the manifold: $\chi = m$. Here m is the conserved topological invariant. It is also referred to as the 2D topological charge of topological defects (TDs) (Mermin, 1979) within the ordering field hosted by the 2D curved manifold. TDs refer to localized topologically protected distortions in a physical field. The key message conveyed by the theorems is illustrated in Fig. 1c, where the 2D manifold exhibits spherical geometry (represented by $g=0$ and $\chi = 2$) enforcing two $m=1$ point defects at the poles in the "axial" ordering field, where the total winding of the manifold equals to two. The two "charge one" point defects resemble point-like bodies. Note that the theorems can be generalized to other abstract (Ramirez and Skinner, 2020) 2D manifolds (e.g., the 1st Brillouin zone surface in crystals). Furthermore, topological concepts developed in 2D, where mathematics could be visualized, could be transferred to higher dimensional manifolds (Singer, 1982)

Above listed theorems are at the heart of the quantum hall effect (Ramirez and Skinner, 2020), representing one of the pioneering discoveries via which topology entered the world of physics, where it might soon become the "queen". Namely, the recent discovery of the Higgs particle confirmed the existence of the Higgs field which supports the viewpoint that physical fields represent fundamental natural entities (Hobson, 2013). This perspective suggests that TDs might embody "particles" of the standard model of physics. Note that such vortex-type theory was first proposed by lord Kelvin (Thomson, 1867) who claimed that atoms (at that time atoms were treated as fundamental particles) are topologically protected knots in the respective physical field. Such simplest knot members are illustrated in **Figures 1d,e,f**. Indeed, "tying a knot" is a metaphor for creating stability. Knots are sturdy in structure and tangled configurations persist much like a knot tied in a shoelace. Along this line of reasoning Skyrme (1962) modelled structures of hadrons and mesons as soliton excitations in the pion-field, where he stabilized these excitations by imposing rather artificial constraints. Topologically related structures (the so called skyrmions) were afterwards predicted or even observed in several other systems, including Quantum Hall magnetism (Brey et al., 1995), Spinor Bose-Einstein condensates (Ho, 1998), helical ferromagnets (Rössle et al., 2006), LC Blue Phases (Meiboom et al, 1981) to mention few of them. A typical 2D skyrmion winding configuration of magnetic skyrmion is depicted in **Figure 1g**. Recent theoretical studies suggest that such 2D structures could be in 3D twisted into complex linked and knotted objects. For example, **Figure 1h** illustrates a "nanoknot" in magnetization field (Sutcliffe, 2017). Similar structures could be realised in optical vortex configuration (Shen et al., 2023). Related knotted and linked topologically

protected structures are present in diverse tube-like structures in nature and seem to be a generic feature of complex pattern close to phase transitions and at the edge-of chaos conditions (Johnson, 2021). They appear at wide range of length scales, e.g., in the range $10^{-10} - 10^{-6}$ m in superfluid vortices, $10^{-2} - 10^2$ m in fluid eddies and tornados, $10^6 - 10^{10}$ m in magnetic flux tubes in universe...

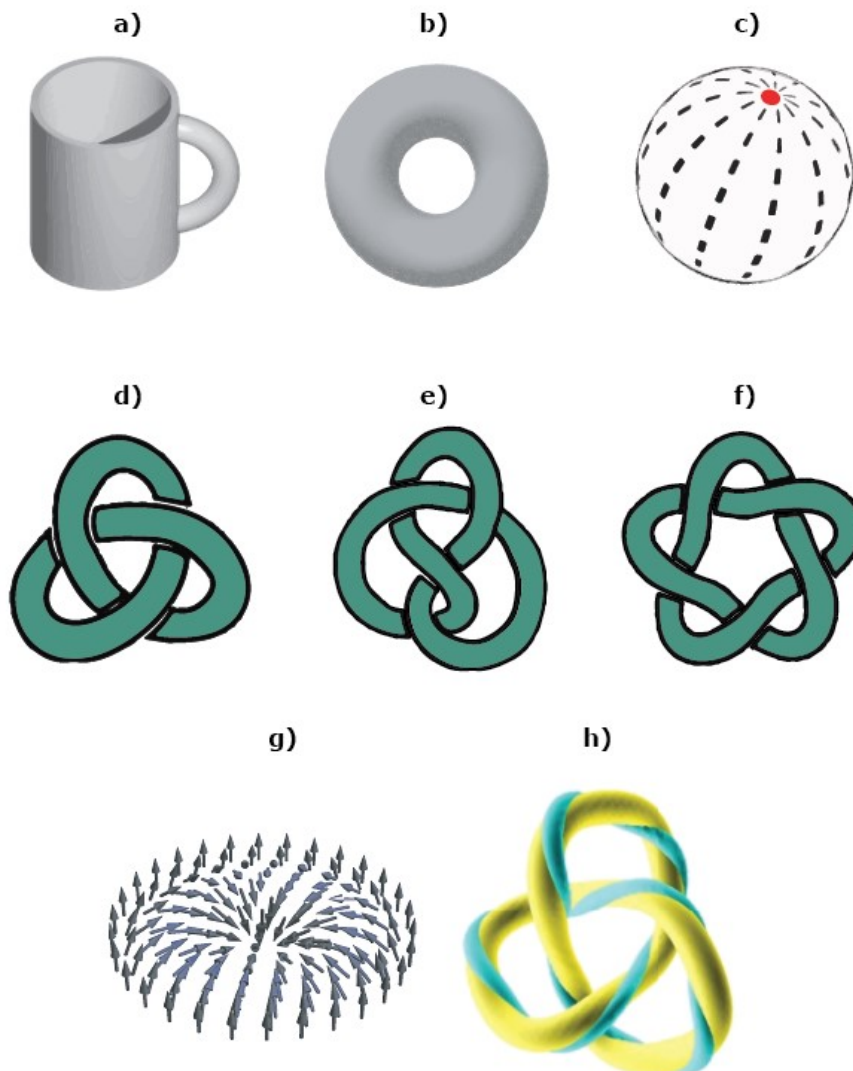


Figure 1. A cup of coffee (a) is topologically equivalent to a torus (b). (c): A sphere hosting a vector field inevitably exhibits topological defects. (d), (e), (f): topologically different knots. (g): 2D skyrmion. (h): A knot in the magnetization vector field.

Particularly adequate systems to carry out controlled and systematic studies of TDs are liquid crystals (LCs). They possess a unique and extraordinary combination of liquid character, crystalline order, softness (i.e. capability to exhibit strong responses even to weak local stimuli), complexity, and optical anisotropy. Owing to these features a rich diversity of TDs could be easily excited, stabilized, manipulated, and observed using relatively simple optic methods (e.g., using polarizing microscopy and laser tweezers). Consequently, LCs provide an excellent testbed system to reveal key features of TDs. Furthermore, TDs



in LCs could serve in various future applications, particularly in photonics and information storage and manipulation.

In this contribution we study configurational transformations of pairs of line defects in nematic LCs confined to a plane parallel cell. We illustrate that in general different reconfiguration channels exist and consequently collided pairs of line defects could in general exhibit qualitatively different post-collision configurations.

2. Methods

Nematic LC phase exhibits long range uniaxial orientational order which is in bulk equilibrium spatially homogeneously aligned along a symmetry breaking direction. At the mesoscopic level it is in general described by the tensor order parameter \underline{Q} . In terms of its eigenvectors \vec{e}_i and eigenvalues λ_i it can be expressed as (Meiboom et al, 1981; Harkai et al., 2020)

$$\underline{Q} = \sum_{i=1}^3 \lambda_i (\vec{e}_i \otimes \vec{e}_i) . \quad (1)$$

This parametrization allows both uniaxial and biaxial states. In the former state, it is conventionally expressed with the nematic director field \vec{n} and the nematic uniaxial order s as $\underline{Q} = s (\vec{n} \otimes \vec{n} - \frac{1}{3} \underline{I})$. The unit vector \vec{n} points along the local uniaxial direction where the states $\pm \vec{n}$ are physically equivalent. Furthermore, the amplitude field $s \in [-\frac{1}{2}, \frac{1}{2}]$ determines the degree of anisotropic order, where $s > 0$ ($s < 0$) reflects prolate (oblate) uniaxial order. Biaxial states could be established at least locally if LC order is distorted. In our simulations, we express \underline{Q} in the Cartesian coordinate frame $(\vec{e}_x, \vec{e}_y, \vec{e}_z)$ as $\underline{Q} = (q_1 + q_2)(\vec{e}_x \otimes \vec{e}_x) + (q_1 - q_2)(\vec{e}_y \otimes \vec{e}_y) - 2q_1(\vec{e}_z \otimes \vec{e}_z) + q_3((\vec{e}_x \otimes \vec{e}_y) + (\vec{e}_y \otimes \vec{e}_x)) + q_4((\vec{e}_x \otimes \vec{e}_z) + (\vec{e}_z \otimes \vec{e}_x)) + q_5((\vec{e}_y \otimes \vec{e}_z) + (\vec{e}_z \otimes \vec{e}_y))$. Quantities $\{q_1, q_2, q_3, q_4, q_5\}$ are variational parameters. This parametrization allows both uniaxial and biaxial states.

In our study we consider nematic order within a plane-parallel cell of thickness h . The identical confining plates are placed at $z=0$ and $z=h$. We prescribe orientational order at these plates. In practice this can be realized, e.g., using AFM scribing method. At the lateral sides we impose the free boundary condition. Nematic order within the cell is calculated by minimizing the nematic free energy.

The free energy F of the system is determined by the integral of the free energy density over the LC body: $F = \int f d^3r$, where (Meiboom et al., 1981; Harkai et al., 2020)

$$f = \frac{1}{2} A_0 (T - T^*) \text{Tr}(\underline{Q}^2) - \frac{1}{3} B \text{Tr}(\underline{Q}^3) + \frac{1}{4} C \text{Tr}(\underline{Q}^2)^2 + \frac{1}{2} L |\nabla \underline{Q}|^2 . \quad (2)$$

Quantities A_0 , B , and C are material constants, T^* is the supercooling temperature of the isotropic phase, and L is the representative nematic elastic constant in the single elastic constant approximation. Note that we use the minimal model to simulate phenomena of our interest.

We introduce the dimensionless temperature $r = (T - T^*) / (T^{**} - T^*)$, where $T^{**} = T^* + B^2 / (24 A_0 C)$ is the superheating temperature, introduce scaled order parameter $\tilde{Q} = \underline{Q} / s_0$, where $s_0 = B / (4C)$, and we scale distances with respect to cell thickness h . The resulting dimensionless free energy density reads (Harkai et al., 2020)

$$\tilde{f} = \frac{r}{6} \text{Tr}(\tilde{Q}^2) - \frac{2}{3} \text{Tr}(\tilde{Q}^3) + \frac{1}{8} \text{Tr}(\tilde{Q}^2)^2 + \left(\frac{\xi_b}{h}\right)^2 |\tilde{\nabla} \tilde{Q}|^2 . \quad (3)$$

Here $\xi_b = 2\sqrt{LC}/B$ is the bare biaxial correlation length and $\vec{\nabla} = h\nabla$. The minimization of the free energy is performed numerically deep inside the nematic phase, far below T^* .

3. Results

We analyse collisions of nematic line defects. 3D nematic LCs could display elementary line defects in orientational order (the so called disclinations) exhibiting winding number $m = \pm 1/2$. This quantity is a topological invariant and is in 2D LCs referred to as the 2D topological charge. It fingerprints the total reorientation of the principal \underline{Q} -eigenvector \vec{e}_1 on encircling by any path the defect center counterclockwise. Note that for uniaxial states it holds $\vec{n} = \vec{e}_1$. Furthermore, one can assign to disclinations also a 3D topological charge q . It reflects number of realizations of all possible \vec{e}_1 orientations sampled on any surface enclosing the whole line defect. Note that in bulk line defects can only form closed loops. On the contrary, in confined geometries they could emanate and terminate on a LC-limiting substrate. Elementary disclinations could exhibit either $|q|=1$ or 0. In the former case the sign of the winding number does not change along the line defect. The far-field of such enclosed defect is distorted and is topologically equivalent to a point defect (monopol) exhibiting topological charge $|q|=1$. Therefore, such defects could strongly interact with their surrounding objects which exhibit coupling with \vec{e}_i . On the other hand, chargeless disclinations, bearing $q=0$, could be surrounded by essentially spatially homogeneous nematic structure. Hence, in general they weakly interact with their surrounding.

In our simulations we impose pairs of $\{m=1/2, m=-1/2\}$ line defects, which are initially essentially parallel, spanning the facing plates of the plane-parallel cell (see Fig. 2a). We enforce such structures by enforcing at each plate a pair of $\{m=1/2, m=-1/2\}$ 2D defects, which otherwise impose planar orientational ordering (i.e., the nematic director field within the plates is confined to the (x,y) planes at $z=0$ and $z=h$). The separation of surface point defects at the bounding surfaces is equal to $r=h/2$. Experimentally, such surface boundary conditions could be realized by AFM scribing method (Harkai et al., 2020). At each plate the lines, designated by unit vectors \vec{e}_0 (at $z=0$) and \vec{e}_h (at $z=h$), connecting the centers of 2D neighbouring defects are initially aligned along \vec{e}_x as shown in **Figure 2a**. We assume that the end-points of line defects are strongly attached to the surface-enforced defect nucleating sites. Afterward we rotate the bottom connection line \vec{e}_0 for the azimuthal angle θ . Figs 2b-2f illustrate representative stages on increasing θ from $\theta = 0$ to $\theta = 2\pi$. In the 1st stage the line defects become elongated, see Fig. 2b. Note that a disclination free energy penalty is for an isolated line defect linearly proportional to its length. To prevent monotonically increasing total length $l^{(tot)}$ on increasing θ the facing disclinations exchange their segments. The reconfiguration process is depicted in **Figures 2c-2d**. At the critical angle $\theta_c = 5\pi/4$ an additional chargeless loop is formed within the (x,y) plane at $z=h/2$ (Fig. 2d), which connects both disclinations running along the cell thickness. The latter two are also chargeless (i.e., their winding number switches its sign on crossing the mid-plane at $z=h/2$). Consequently, the total length of disclinations reaches the maximum at $\theta_c = 5\pi/4$ and on further increasing θ in the interval $\theta \in [\pi, 2\pi]$ the total disclination length is monotonically decreasing, reaching the minimal length $l^{(tot)} \sim 2h$ at $\theta = 2\pi$. The final configuration (**Figure 2f**) is identical to the initial configuration (**Figure 2a**). Therefore, the structural transformations exhibit periodic behaviour with the period 2π on increasing θ . Such behaviour is realized in thick enough cells.

Next, we analyse the rotation-imposed reconfiguration in a thinner cell where characteristic stages are shown in **Figures 3**. On increasing θ the total length of disclinations increases in the interval $\theta \in [0, \theta_c]$, where a characteristic pattern is shown in **Figure 3b**. However, at θ_c , the charged disclinations collide and rewire into two chargeless configurations. The latter two connect the nearby surface-imposed 2D point defects. In order to reduce their length, they become relatively strongly confined to the bounding substrates,

see Figs. 3c and Fig. 2f. Therefore, the total length of disclination at $\theta = 2\pi$ equals roughly $l^{(tot)} \sim 2h$. Furthermore, $l^{(tot)}$ exhibit weak $l^{(tot)}(\theta)$ dependence in the regime $\theta > \theta_c$.

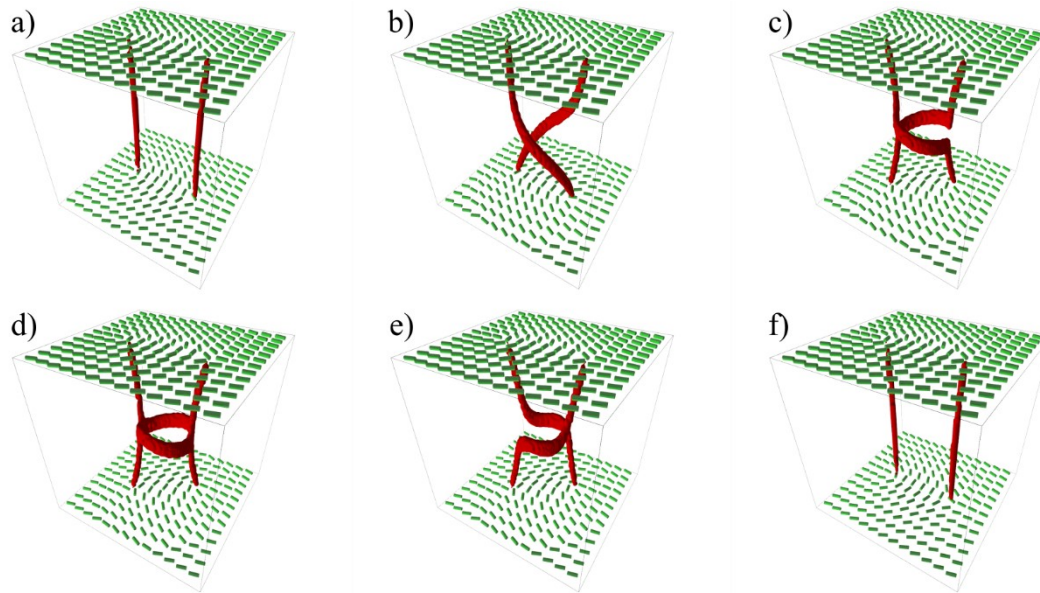


Figure 2. Structural reconfiguration of $\{1/2, -1/2\}$ topological line defects on increasing θ in thin cells. (a) Initial structure at $\theta = 0$. b), (c), (d), (e): intermediate states on progressively increasing θ . (f): Final state reached following $\theta = 2\pi$ rotation.

In this case the system does not exhibit periodic behaviour on increasing θ .

4. Discussion and conclusions

We studied transformations of disclinations in nematic LCs, which correspond to line defects in the molecular field. In a bulk equilibrium, the field exhibits spatially homogeneous uniaxial orientational order along a symmetry-breaking direction. The degeneracy of competing equilibrium configurations enables the existence of topological defects. We focused on line defects. We stabilized them by appropriate surface boundary conditions. By relative rotation of confining plates, we enforced structural transformation of pairs of disclinations. We demonstrated that disclinations behave like elastic bodies that can recombine in different structures. In our study, the initial (non-rotated) structure possesses two charged disclinations exhibiting winding numbers $m = -1/2$ and $m = 1/2$. The far field of such closed disclinations would resemble point defects bearing 3D topological charges $q = -1$ and $q = 1$, respectively. Therefore, the total topological charge of the system equals zero. In addition, the total winding within each (x, y) plane equals zero. In our simulations, we demonstrated two qualitatively different rotation-driven reconfigurations of disclinations. In all cases the topological conservation rules were obeyed: i.e., each (x, y) plane and also the whole system were topologically neutral.

Note that physics of TDs is strongly dominated by topology which is independent from system's microscopic details. Therefore, lessons learned from detail studies in one system, which is experimentally accessible, might gain understanding on behaviour of TDs in systems, where experimental studies of TDs are difficult (e.g., study of cosmic strings in space-time fabric). Our study reveals that interacting line defects in flat geometry could not form

complex knots as first suggested by Kelvin (see **Figures 1d,e,f**). However, more complex structures could be stabilised by including into the play geometrical curvature. For example, in our setting this could be achieved by immersing a toroidal colloid into the nematic fluid, where the colloid's surface would impose isotropic tangential anchoring (i.e., all nematic director field orientations within the colloid's surface are energetically equivalent). Namely, torus possesses surface regions exhibiting positive and negative Gaussian curvature K_g . Recent studies in 2D curved manifolds (Mesarec et al., 2016) reveal that surface regions exhibiting $K_g > 0$ ($K_g < 0$) attract TDs bearing $m > 0$ ($m < 0$). Therefore, one expects that chargeless loops, which possess both $m > 0$ and $m < 0$ segments could wind around torus geometry. We believe that by imposing strong enough excitations (for instance by switching on/off a strong enough AC external electric field, where one could vary the field amplitude and frequency) one could stabilize topologically different "torus knots" (Singer, 1982). This is the goal of our future research activity.

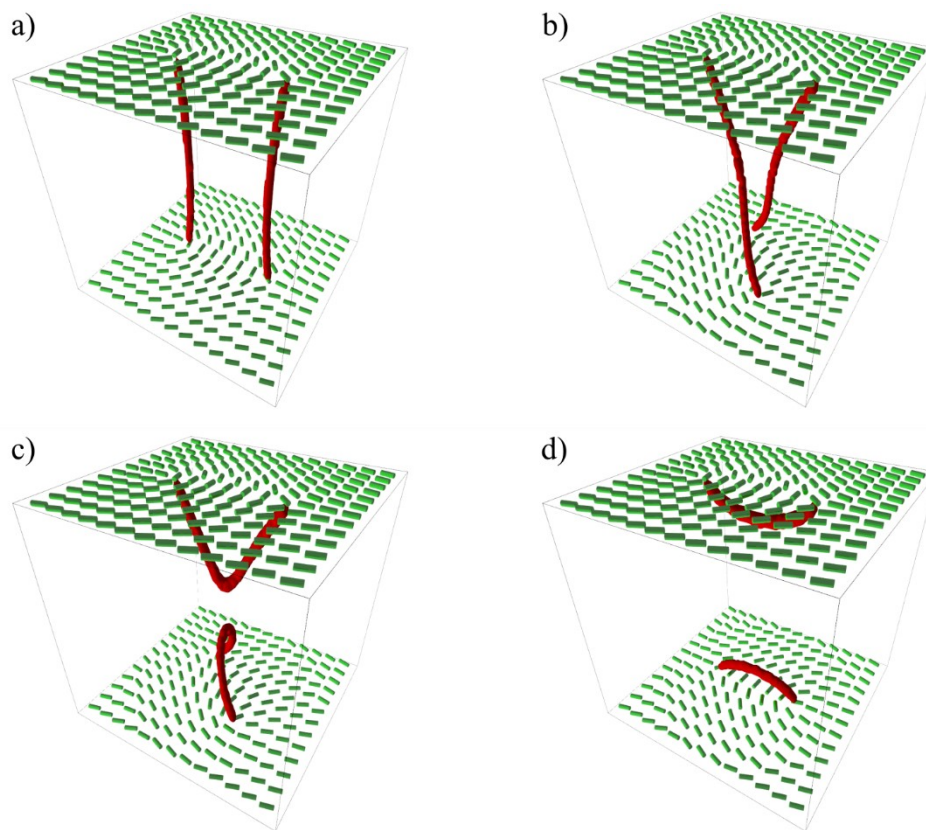


Figure 3. Structural reconfiguration of $\{1/2, -1/2\}$ topological line defects on increasing θ in thick cells. (a) Initial structure at $\theta = 0$. (b), (c): intermediate states on progressively increasing θ . (d) Final state reached following $\theta = 2\pi$ rotation.

Funding: This research was supported by Slovenian Research Agency grants P1-0099 and J1-2457.

Conflicts of Interest: The authors declare no conflict of interest.



References

1. Brey L, Fertig HA, Côté R, MacDonald AH. Skyrme Crystal in a Two-Dimensional Electron Gas. *Phys. Rev. Lett.* 1995; 75: 2562. DOI: <https://doi.org/10.1103/PhysRevLett.75.2562>
2. Harkai S, Murray BS, Rosenblatt C, Kralj S. Electric field driven reconfigurable multistable topological defect patterns. *Phys. Rev. Res.* 2020; 2:013176. DOI: <https://doi.org/10.1103/PhysRevResearch.2.013176>
3. Ho TL. Spinor Bose Condensates in Optical Traps. *Phys. Rev. Lett.* 1998; 81: 742. DOI: <https://doi.org/10.1103/PhysRevLett.81.742>
4. Hobson A. There are no particles, there are only fields. *Am. J. Phys.* 2013; 81: 211. DOI: <https://doi.org/10.1119/1.4789885>
5. Johnson PL. The squeezes, stretches, and whirls of turbulence. *Physics Today.* 2021; 74: 46. DOI: 10.1063/PT.3.4725
6. Kamien RD. The geometry of soft materials: a primer. *Rev. Mod. Phys.* 2002; 74: 953. DOI: <https://doi.org/10.1103/RevModPhys.74.953>
7. Meiboom S, Sethna P, Anderson PW, Brinkman WF. Theory of the Blue Phase of Cholesteric Liquid Crystals. *Phys. Rev. Lett.* 1981; 46: 1216. DOI: <https://doi.org/10.1103/PhysRevLett.46.1216>
8. Mermin N. The Topological Theory of Defects in Ordered Media. *Rev. Mod. Phys.* 1979; 51: 591. DOI: <http://dx.doi.org/10.1103/RevModPhys.51.59>
9. Mesarec L, Gózdź W, Iglíč A, Kralj S. Effective topological charge cancelation mechanism. *Sci Rep.* 2016; 6:1-12. DOI: <https://www.nature.com/articles/srep27117>
10. Ramirez AP, Skinner B. Dawn of the topological age? *Physics Today.* 2020; 73: 30; DOI:10.1063/PT.3.4567
11. Rössler UK, Bogdanov AN, Pfleiderer C. Spontaneous skyrmion ground states in magnetic metals. *Nature.* 2006; 442: 797. DOI: <https://doi.org/10.1038/nature05056>
12. Shen Y, Bingshi Yu, Haijun Wu, Chunyu Li et al. Topological transformation and free-space transport of photonic hopfions. *Advanced Photonics.* 2023; 5: 015001. DOI:<https://doi.org/10.1117/1.AP.5.1.015001>
13. Singer IM. Differential geometry, fiber bundles and physical theories. *Physics Today.* 1982; 35: 41. DOI: <https://doi.org/10.1063/1.2914967>
14. Skyrme THR. A unified field theory of mesons and baryons. *Nucl. Phys.* 1962; 31: 556. DOI:[https://doi.org/10.1016/0029-5582\(62\)90775-7](https://doi.org/10.1016/0029-5582(62)90775-7)
15. Sutcliffe P. Skyrmion Knots in Frustrated Magnets. *Phys. Rev. Lett.* 2017; 118: 247203. DOI: <https://doi.org/10.1103/PhysRevLett.118.247203>
16. Thomson V. On vortex atoms. *Philos. Mag. Ser.* 1867; 4: 34. DOI: <https://doi.org/10.1080/14786446708639836>